CORROSION IN SPACE

A. de Rooij
Head of Materials Technology Section
Product Assurance and Safety Department
Materials and Components Technology Division
European Space Agency
European Space Technology and Research Centre
Noordwijk, The Netherlands

Keywords:
atomic oxygen, corrosion, space, low earth orbit, LEO, ATOX, flight testing, on-ground testing

Abstract
The corrosion in space is described by the effect of atomic oxygen on several materials. The metal which was most affected is silver. Silver oxidises according to a linear-parabolic law and due to the thermal stresses the oxide layer continuously breaks up, resulting in a linear degradation.
Atomic oxygen not only attacks materials in the line of sight of the ram flux, but also by reflected atomic oxygen.
Many materials form an adherent oxide layer, such as Cu, Al and stainless steel and are as such protected once this oxide layer is formed. Some materials have a volatile oxide such as Osmium and many polymers materials. They show a linear behaviour.

1 INTRODUCTION

Corrosion in the space environment can happen during several occasions. In satellites, manned and unmanned, the environment is present which can contribute to all kinds of corrosion. The presence of electrolytes in batteries and/or cooling loops can cause galvanic corrosion, general corrosion and stress corrosion. These corrosion types are fully equivalent to ones find on ground. In the life of a spacecraft most of the dangers of corrosion happens on ground during manufacturing, assembly, testing and or storage. The one corrosion type which is usually not found on ground is corrosion by atomic oxygen (ATOX). ATOX is considered as one of the most serious hazards to spacecraft materials and is present at altitudes between 200 and 700 km.
The degrading environment for spacecraft materials includes atomic oxygen, Ultraviolet (UV) radiation, ionizing radiation, ultrahigh vacuum (UHV), charged particles, thermal cycles, electromagnetic radiation, micrometeoroids, and man-made debris, micrometeoroids and orbital debris. Synergistic or separate interactions in this environment, the spacecraft materials might suffer corrosion, erosion, structure modification and surface roughening, which can degrade the optical, thermal, electrical and mechanical properties.

2 WHAT IS ATOMIC OXYGEN

ATOX is produced by the photo-dissociation of molecular oxygen in the upper atmosphere by solar radiation of wavelength less than or equal to 243 nm [1]. It is the main constituent of the residual atmosphere in Low Earth Orbit (LEO) as illustrated in figure 1 [2]. The oxygen atoms have a density of 10^7 to 10^8 atoms/cm^3 at International Space Station (ISS) altitude (around 400 km) with a thermal energy of approx. 0.1 eV.

The orbital atomic oxygen density can be calculated with the aid of the MSIS-86/CIRA Neutral Thermophere Model of Hedin[3].

Referring to figure 1 one can see the dominant atmospheric constituent concentrations as a function of altitude. Space vehicles are orbiting with a velocity of 7.78 to 8 km/sec at those altitudes. For satellite-gas collision interactions, this orbital velocity corresponds to impact gas energies of 0.34, 4.40 and 5.03 eV for hydrogen, nitrogen and oxygen atoms, respectively.
Concentrating only on the O-atoms and taking into account the solar activity the maximum and minimum atomic oxygen density as function of altitude is shown in figure 2. The atomic oxygen flux depends on the altitude, the solar activity, the orbital inclination and the time of year. The collision with the external surfaces of space vehicles, orbiting at a velocity of 8 km/s, results in a ram flux of 10^{14} -10^{15} O-atoms/(cm^2.s).

3 ATOMIC OXYGEN EFFECTS

A number of processes can take place when oxygen atoms strike a spacecraft surface at orbital velocities. These include chemical reaction with surface atoms or adsorbed molecules, elastic scattering, scattering with partial or full thermal accommodation, recombination, or excitation of ram species.
The chemical reaction of ATOX with a surface may cause the formation of volatile oxides from polymers, carbon, and osmium; or oxides which do not adhere very well to the surface and tend to spall, as in case of silver. Volatile and spalling oxides contribute to the erosion of the surface. In several cases the oxide remains adhered to the surface and is not porous. In these cases the surface oxide is protective and the underlying material will not erode away. This is the case for most metals such as aluminium, copper, steel and also for silicon. The oxidation product for most polymers is a gas and erosion results.
The factors that may influence the erosion yield of materials in space are impact angle, material temperature, oxide spalling, ATOX flux, ATOX fluence, synergistic solar radiation, and ATOX impact energy. Following the sequence of Banks and Rutledge [4]:

3.1.1 ATOX fluence

The erosion yield of Kapton due to space exposure reveals no pronounced dependence upon ATOX flux or fluence based on information from Space Transportation System (STS) flight 3, 4, 5, and 8. The corrosion of silver slows down with increasing ATOX fluence due to the protective oxide layer when still on the surface. No dependence on ATOX flux is seen based on STS-8, 41 and Long Duration Exposure Facility (LDEF) information.

3.1.2 ATOX impact energy

The dependence of erosion yield upon impact energy has been measured both in the ground-based laboratory and in space simulation. In the simulations, an erosion yield dependence of Kapton to energy E can be expressed as Yield=$E^{0.68}$ [5]
The energy of atomic oxygen arrival may have a significant influence on the erosion yield of materials relative to Kapton H. At thermal energies in RF plasma ashers, materials with high chlorine or fluorine atomic contents have anomalously high

erosion yields relative to in the LEO environment. However, at hyperthermal energies of ~70 eV, there does not seem to be a clear or simple chemical composition dependence upon the erosion yields.
The corrosion of silver has been measured in ground ATOX simulators using different energies and during space flight and no effect is seen. The energies encountered during these tests are generally too low to have an effect on the metal bond.

3.1.3 Material temperature

The temperature range in the laboratory experiments is too small for evaluation of Kapton, Mylar and Tedlar to identify any dependence of the erosion yield upon material temperature.
Corrosion of metals is related to diffusion phenomena of either metal ions of oxygen ions through the oxide layer. This process is temperature dependent. In the case of silver the material temperature plays also a role in the phase change between AgO and Ag_2O which occurs around 100°C. This was observed several times during ground testing in oxygen plasmas.
Also transformation temperatures of the oxides such as melting points, sublimation temperatures play an important role. The large atomic oxygen effect on osmium can be explained by the low melting point of OsO_4 (assumed it is formed) of 40°C. It starts to sublime below its melting point (temperature in LEO is +l00/-100°C).

3.1.4 Thermal stresses

Thermal stresses occur in the LEO orbit on the outer surface of satellites due to periodic in and out of the sunshade during orbiting. At LEO this occurs each 90 minutes and is roughly +100°C to -100°C. This temperature change causes thermal stresses in materials and the difference in CTE will cause spalling of the oxide layer present on metal surfaces and results in constantly exposing fresh material to the atomic oxygen environment.

3.1.5 Synergistic solar radiation

Synergistic effects such as temperature and ultraviolet exposure may be important for some materials and not for others. In general metals are not affected by UV exposure.

3.1.6 Impact angle

The effect of ATOX impact angle for Kapton and Mylar in space shows that the rate of material recession depends on the impact angle with respect to the surface normal, θ as ($\cos\theta$).

3.1.7 Indirect attack

Indirect attack of silver by reflected atomic oxygen was seen on STS-5 where the rear side of the silver samples were oxidised to the amount of 25-50% of that of the front side. Experiments on Kapton were performed by Banks et.al. [6] also showed the same effect

3.2 Atomic Oxygen on metals

Experiments on metals were carried out during many STS flights, on LDEF, Eureca and on ground. The majority of the experiments were conducted on silver, while at the time of the Hubble Space Telescope development silver was used as solarcell interconnectors. On-ground experiments were conducted in line with these ones and extended with other metals.

The oxidation of silver in atomic oxygen is essentially linear-parabolic as postulated by De Rooij [7] and experimentally confirmed by Chambers et.al. [8]. The silver oxidises according to described equation until internal stresses in the oxide layer either to mechanical or thermal excursions causes the oxide layer to crack and eventually spall and flake off, leaving bare silver exposed to atomic oxygen again. This process repeats itself until the silver is completely oxidised. The silver oxide is very fragile and porous with a volume ratio of the oxide to the metal of >2. The typical oxide thickness at which the spalling and flaking occurs is around 0.5 μm. This periodic flaking of the oxide layer results in an overall linear degradation of the silver. During the relative short Space shuttle missions the silver reduced 3 to 4.5 μm in thickness depending surface normal to the velocity vector.
An oxide layer model was developed to predict the silver oxidation by atomic oxygen in the ISS orbit. (figure 3). The mechanism of oxide growth at increased temperatures is diffusion through the oxide layer. As the diffusion is a temperature-controlled process, the observation of a substantial amount of oxidation at room temperature indicates a different oxidation process or at least a parallel process capable of oxidising the metal in a parabolic manner and operational at low temperatures. The process responsible for the low temperature oxidation is known as gas flow through micro-pores.
Several mechanisms of gas transport trough micro-pores can occur. These are free molecular flow (Knudsen flow), molecular flow, viscous flow and surface diffusion. At very low pressures where the mean free path of the oxygen atoms is larger than the dimensions of the pore, the wall collisions within the pore are more frequent than collisions between other oxygen atoms. This regime is called the free-molecular flow regime. The density of O-atoms in low earth orbit is approx. 10^8 atoms/cm^3 and the mean free path is calculated ad 10^7 μm which is much larger then the expected pore dimension.
The number of atoms flowing through a pore is determined by the conductance of that pore. These are two aspects:

1) The rate at which atoms enter the pore
2) The probability that these atoms are transmitted though the system.

A gas with a density of n_1 at the entrance of a pore and a backflow at the other side gives a gasflow F_k of

$$F_k = \omega \bar{\upsilon} (n_1 - n_2) \tag{1}$$

where ω = a dimensionless probability factor
$\bar{\upsilon}$ = the mean velocity of the atoms in the pore

The atoms entering the pore loose their velocity due to scattering in the pores during the first wall collisions. Their speed is than reduced to $\bar{\upsilon}$
The expression for n_1 is then

$$n_1 = \frac{Nv}{\bar{\upsilon}} \tag{2}$$

where N = the atomic oxygen density
v = velocity of the spacecraft
Nv = ϕ = the flux of atomic oxygen on the spacecraft

$$\bar{\upsilon} = \sqrt{\frac{8RT}{\pi M}}$$

from gas kinetic theory (3)

R = gas constant
T = temperature
M = molecular mass

The probability factor ω depends on the geometry of the pore and is given by the Clausing factor

$$\omega = \left[1 + \frac{3}{16}\frac{L_r H}{A}\right]^{-1} \tag{4}$$

where L_r = the real length of the micropore
H = perimeter of the micropore
A = cross sectional area of the micropore

The pores have a certain path through the oxide layer and this can be related to the straight direct path y, which is the oxide thickness, by the tortuosity τ.

$$\tau = \frac{L_r}{y} \tag{5}$$

Only a percentage ε of the surface consists of open pores where the Knudsen flow can take place.
In summary we can write for the flow of oxygen atoms through porous layer by substituting eq. 2, 3 and 5 in eq. 1:

$$F_k = \varepsilon\left[1 + \frac{3}{16}\frac{Hy\tau}{A}\right]^{-1}\left\{\phi - n_2\bar{\upsilon}\right\} \tag{6}$$

Diffusion through short circuits and lattice is governed by the concentration difference of the diffusion atoms at both sides of the porous layer. At the front side the density is given by eq. 2. At the metal side the density is n_2.
The differential flux of atoms through the oxide layer (with the exception of the pores) is then written as:

$$F_d = \frac{D(1-\varepsilon)}{y}\left\{\frac{\phi}{\bar{\upsilon}} - n_2\right\} \tag{7}$$

where D =diffusion coefficient = $D_0 \exp\left(\frac{-Q}{RT}\right)$

The oxygen atoms reaching the metal surface will finally react with the base metal and form the oxide. This type of reactions is usually linear and with an oxide flux of:

$$F_o = Kn_2 \tag{8}$$

where K = rate of metal oxidation = $K_0 \exp\left(\frac{-Q}{RT}\right)$

For a steady state situation the oxygen flux through the pores F_k and from the diffusional transport F_d must be equal to the oxide flux F_o produced by the oxidation:

$$F_k + F_d = F_o \tag{9}$$

The unit for the oxide flux F_o is related to the oxide growth rate by

$$\left(\frac{dy}{dt}\right)_{ox} = C\Omega_r F_o \tag{10}$$

Where
C = conversion factor from atoms/cm^3 to cm^3 metal-oxide
= 1.70520 10^{-23} for silver
Ω_r = real volume ration oxide/metal due to porosity

$$\Omega_r = \frac{\Omega_{th}}{(1-\varepsilon)} \tag{11}$$

In which Ω_{th} = theoretical volume oxide/metal ratio = 1.6 for silver

Substituting eq. 6, 7 and 8 into eq. 9 enables us to express the generally unknown n_2, in the gasflow and diffusion expressions and using this in eq. 10 one obtains the master equation for the oxide growth governed by the gasflow and diffusion transport mechanism through the oxide layers.

$$\left(\frac{dy}{dt}\right)_{ox} = \frac{CK\dfrac{\Omega_{th}}{(1-\varepsilon)}\dfrac{\phi}{\bar{\upsilon}}}{1+\dfrac{Ky}{\dfrac{\varepsilon\bar{\upsilon}y}{1+\dfrac{3Hy\tau}{16A}}+D(1-\varepsilon)}} \tag{12}$$

Equation 12 can solved using standard methods and after some algebra this results in:

$$\frac{\Omega_{th}CK\phi.t}{\bar{\upsilon}(1-\varepsilon)} = y^2\frac{KP_c}{2W} + y\left\{1+\frac{K}{W}-\frac{KP_cD_\varepsilon}{W^2}\right\} - V\left\{\frac{K}{W}-\frac{KP_cD_\varepsilon}{W^2}\right\} \tag{13}$$

Where
$$P_c = \frac{3H\tau}{16A}$$
$$D_\varepsilon = D(1-\varepsilon)$$
$$W = \varepsilon\bar{\upsilon} + P_cD_\varepsilon$$
$$V = \frac{D_\varepsilon}{W}\log\left(1+\frac{Wy}{D_\varepsilon}\right)$$

This general solution reduces to the well known linear-parabolic equation when gasflow is absent:

$$\frac{y^2}{D} + \frac{2y}{K} = \frac{2\Omega_{th}C\phi.t}{\bar{\upsilon}} \tag{14}$$

In case diffusion is absent equation 13 reduces to

$$y^2 P_c + \frac{2\overline{\upsilon}\varepsilon}{K} y = \frac{2\Omega_{th} C \varepsilon \phi . t}{1-\varepsilon} \qquad (15)$$

It may be noted that also the gasflow equation 15 is linear-parabolic. The temperature dependence of eq. 15 is weak and only present in the linear part, meaning when *y* is very small. With thicker oxide layers the gasflow through the pores behaves parabolic because of the collisions of the atoms with the wall of the pore. The diffusion equation 14 has the temperature dependence both in the linear and in the parabolic part. It demonstrates that at low temperatures the gasflow through the pores is the dominating process, while at high temperature the diffusion is rate controlling.

At a typical ISS orbit the silver loss due to oxidation is calculated as 11.5 μm per year with an oxide thickness of 23 μm when no spallation is assumed. When complete flaking is assumed the maximum loss is 300 μm per year.
The solar cell interconnectors are typically silver foil with a thickness of 20 μm. A stress relief loop is formed in the foil to accommodate for the displacements between the solar cells. This out-of plane-loop is mechanically formed. The atomic oxygen effect is usually most pronounced on out-of-plane stress relief loops. In this area the manufacturing stresses and the stresses as a result of the temperature excursions are large. Past experience showed that in these areas the oxide layer tends to flake off and a fresh surface is exposed to the atomic oxygen environment. On flat surfaces this effect is less pronounced while there mainly the difference in volume between the oxide and the parent metal is responsible for cracking of the oxide layer. The largest effect is seen on the ram surface. However, also on surface not directly exposed to the ram fluence, atomic oxygen oxidation is seen as evidenced by the fact that the rear side of the silver samples were always oxidized although to a lesser extend. In general this effect is about 25-50% of the front side of the exposed samples.

On way to protect the silver of being oxidized by atomic oxygen is by plating with gold. Gold is supposed to not be affected by atomic oxygen and when very thin it also does not influence the working of the stress relief loops. As with all protective coatings they should remain intact. Deformations required for manufacturing or during services can jeopardize the integrity of coatings and make them unreliable.
The gold plated interconnectors were finally rejected for out-of-plane stress relief loops because it was impossible to apply a gold coating with such properties that it remained intact after forming the stress relief loop. It was seen several times that these gold layers were either cracking (especially in the out-of-plane loop) or contained small pinhole type defects.
Through these defects the underlying silver was oxidised. Large holes under the gold plating were created and silver-oxide was found at the surface.
In the low Earth orbital environment, one should not use materials which suffer from atomic oxygen corrosion on external surfaces nor on surfaces which can be reached by atomic oxygen neither should one protect materials such as silver by materials with low erosion or corrosion yields.

Other metals investigated are Cu, Au, Al, stainless steel, Ta, Al alloys and Mo. These materials were exposed with and without coatings, such as silicones. Cu was exposed during the LDEF mission and showed a severe darkening (dark red) of the surface, changing the optical properties significantly. The cuprous oxide was adherent to the surface. Other groups investigated Os, Pt, Ni, Fe-alloys and carbon.

3.3 Atomic Oxygen on non-metals

Glasses and ceramics which are based on oxides are expected not to oxidise further. No degradation is reported.

3.4 Atomic Oxygen on organic materials

It is well documented through orbital and ground measurements that most hydrocarbon polymers and active metals are highly reactive towards the orbital atomic oxygen. Materials containing silicones, fluorides, oxides and noble metals are believed to be moderately inert for short exposures to atomic oxygen; however, samples recovered from LDEF indicate that many materials are severely degraded on long-term exposure to atomic oxygen

The tests conducted by Miller et.al. in [9] indicate that environments which produce synergistic effects with regard to the magnitude of erosion by atomic oxygen exposure are not the same for each polymer. Each polymer appears to be sensitive to a different component of the environment. Predicting the atomic oxygen durability of a material in the space environment can be a very complex task complicated by the fact that each material may be sensitive to a different synergistic component in the environment.

3.5 Atomic Oxygen on lubricants

Atomic oxygen can gives serious problem in wear-life of MoS_2 lubricant. For MoS_2 films sputter-deposited at 50–70 °C, friction measurements showed a high initial friction coefficient (up to 0.25) for MoS_2 surfaces exposed to atomic oxygen, which dropped to the normal low values after several cycles of operation in air and ultrahigh vacuum.[10]. Mo-oxide, once formed, act as a protective layer against further atomic oxygen attack. Delamination of cracking of the oxide layer caused by operation of the parts can reduce the wear-life of the film.

3.6 Trapping of Atomic Oxygen between Defected Protective Surfaces

Although atomic oxygen attack on internal or interior surfaces may not have direct exposure to the LEO atomic oxygen flux, scattered impingement can have can have serious degradation effects where sensitive interior surfaces are present.

Atomic oxygen not only attacks surfaces which are exposed directly to the flux, also surfaces not directly exposed, but in one way or another accessible to the atoms can be oxidised. An example is the thermal blanket covering the Ultra High Cosmic Ray (UHCR) experiment exposed on Eureca. This blanket consists of a four layers with Teflon as outer layer and a silver and Inconel as internal layers with black paint at the back side. The internal silver was oxidised by ATOX through a hole created by a micro-meteorite.

The lack of atomic oxygen protection provided by the aluminized Kaptoṇ blanket cover for the ISS photovoltaic arrays box cushion is thought to be due to due to the trapping of atomic oxygen between the two aluminized surfaces on the 0.0254 mm thick Kapton blanket. Defects in the space exposed aluminized surface allow atomic oxygen to erode undercut cavities.

Prediction of the attenuation of the oxidizing effects of the atomic oxygen flux can be reasonably achieved through the use of Monte Carlo computational modelling. A two-dimensional Monte Carlo model has been developed which has been used for such predictions. [11]

4 TESTING

The atomic oxygen erosion measurement techniques should follow the protocols designated in the ASTM procedure E 2089-00 for Standard Practices for Ground Laboratory Atomic Oxygen Interaction Evaluation of Materials for Space Applications[12].

4.1 Flight testing

Surfaces of materials used in the Space Shuttle Orbiter payload bay and exposed during STS-1 through STS-3 were examined after flight.[13]
Films made of carbon, silver, and osmium, were exposed during the Shuttle STS-4 mission examined for the anticipated reaction with atomic oxygen[14]
Bare silver samples and partly coated silver samples were exposed to low earth orbit conditions during Shuttle flights STS-8 and STS-17.[15] The influence of atomic oxygen on the amount of erosion-corrosion of metal surfaces, especially silver, was examined. Protection schemes for silver were also investigated.
The STS Mission 46 carried in orbit a large number of experiments collectively grouped under the designation of Evaluation of Oxygen Interaction with Materials (EOIM-III)-third phase
Some results have been given by the Solar Max (1984) returned materials, but not as a planned experiment.
LDEF was a large cylindrical space experiment rack that exposed various material samples to outer space for about 5.7 years. It was retrieved from space in 1990.
The retrieval of Eureca gave the opportunity to study the effects of atomic oxygen on exposed spacecraft surfaces in Low Earth Orbit. Large areas of identical surface materials, were exposed during the 1992-1993 period,
The first solar array of Hubble Space Telescope was returned after 3 years of operation. All materials presents were examined including Ag, Inconel, stainless steel, copper and kapton.
Samples of Kapton H were transported to the International Space Station attached to the exterior of the ISS during the STS 105 Shuttle mission. The materials were retrieved during the STS-114 Shuttle mission.
There have been five Materials International Space Station Experiment (MISSE) passive experiment carriers (MISSE 1-5) to date that have been launched, exposed in space on the exterior of International Space Station (ISS) and than returned to Earth for analysis.
The Material Exposure and Degradation ExperimenT (MEDET) will actively monitor material degradation dynamics in low Earth orbit and acquire information about the International Space Station environment in terms of contamination, atomic oxygen, ultraviolet and X-ray radiation, micrometeoroids and debris.

4.2 Ground based Atomic Oxygen testing

The existing AO beam sources can be classified according to the physical process involved in dissociation of molecular oxygen: laser-induced breakdown, microwave

dissociation, ion neutralization, electron-simulated desorption, and photo-dissociation. [16]
AO sources have been created and are being used in many research centres around the world: NASA MSFC, NASA JPL, Montana State University (USA), ESTEC (Netherlands), ONERA/DESP (France), ITL/UTIAS (Canada), Kobe University (Japan),

4.2.1 RF Atomic Oxygen Plasma (plasma etcher)

For ground-based AO this study used a 13.56-MHz Plasma asher operated with oxygen or air. This type of asher produces ATOX by the use of a low pressure, radio-frequency induced, gaseous discharge. The plasma contains multiple potential aggressor such as atoms, atomic ions, molecular ions, exited species, ozone etc. It combines the oxidation reactions with possible influences of UV photons, target heating, electrical charging effects etc…

4.2.2 End Hall ion source

The End-Hall Ion Source is a permanent magnet ion source. It produces a beam of almost exclusively O_2^+ with negligible O^+ or O^{++} ions. The energy distribution contained two distinct energy peaks (one at ~40 eV and one at ~85 eV) which resulted in an average energy of ~70 eV. A water-cooled thermal radiation shield can be used to shield samples located downstream and prevent sample heating from the heat radiated by the end Hall source cathode

4.2.3 Plasma neutralization

It utilizes a microwave power source to excite O_2 to produce oxygen plasma. The plasmas become a beam under the effect of an electromagnetic field. The oxygen plasma beam is accelerated by an electric field which is produced by negatively biased metallic plate. The accelerated oxygen plasma beam collides with the plate, and oxygen plasmas are neutralized by the negative charges on the plate and rebounded to form neutral ATOX beam with impingement kinetic energy,

4.2.4 Pulsed laser breakdown

The source concept selected for ATOX is based on the Laser Pulse Induced Breakdown (LPIB) principle, studied and experimented in the USA by Physical Sciences Inc. (PSI, Andover, MA). First, molecular oxygen is forced through the throat of a nozzle, in the form of gas puffs generated by a fast-switching molecular beam valve. After partial fill of the nozzle, a high power beam from a pulsed CO_2 laser
(wavelength 10.6μm) synchronised with the valve is focused onto the injected gas. This produces breakdown and dissociation of the gas into a very hot (>20,000K) plasma. The detonation creates a blast wave that propagates through the nozzle with, as well known from the theory of gas dynamics, conversion of the plasma thermal energy into directed velocity. The cooling of the expansion allows the plasma to charge neutralise into oxygen atoms, but the expansion rate is kept sufficiently high, and the density sufficiently low, to prevent recombination of these atoms into molecules. A thermally cold (low spread in random velocity - meaning a couple of thousand Kelvin) ATOX beam with high directed energy finally exhausts the nozzle and propagates towards the samples.
A regulator system is used to perform thermal cycling between -150°C to +150°C with a slope of 10°C.min-1 by using liquid nitrogen as a cold source and a heating

resistor which is incorporated into the sample holder. Furthermore the sample holder can be rotated up to a beam axis angle of attack of 70°.

5 CONCLUSION

The effect of atomic oxygen on surfaces in laboratory experiments might be different from the effect encountered during low earth orbit exposure. During orbit the exposed samples undergo a thermal cycling sequence of +100/-100°C. This might have a detrimental effect on some oxides. The simultaneous action of atomic oxygen attack and thermal cycling might be compared with such effects as static stress and corrosion (stress corrosion) and fatigue and corrosion (corrosion fatigue), where the result of the combined action is more than the sum of the separate effects. The pure metals are virtually unaffected by thermal cycling itself, also the effect of atomic oxygen on metals such as Au, Pd and Al is in the line of expectation compared to the sputtering yields under 20 KeV O_2^+ bombardment. Following these yields, the value for silver (and osmium) has to be in the same order of magnitude. However, a dramatic effect on silver and osmium is observed in LEO, which is due to the combined action of atomic oxygen attack and thermal excursions. Therefore, on ground testing of materials of materials for LEO behaviour should always incorporate both atomic oxygen attack as well as thermal cycling. To predict materials performance in low earth orbit, one must accurately simulate the conditions of the low earth orbit environment or at least understand how the performance of materials under simulated conditions relates to that in space.

6 REFERENCES

1. Bruce A. Banks, et al., *Atomic Oxygen Effects on Spacecraft Materials.* NASA/TM—2003-212484, 2003.
2. Daniel R. Peplinski and Graham S. Arnold. *INTRODUCTION TO: SIMULATION OF UPPER ATMOSPHERE OXYGEN SATELLITE EXPOSURE TO ATOMIC OXYGEN IN LOW EARTH ORBIT*. in *13th Space Simulation Conference*. 1984. Orlando, Florida.
3. Hedin, A.E., *MSIS-86 Thermospheric Model,*. J. Geophys. Res. , 1987. **A5(92)**: p. 4649.
4. Banks, B.A. and S. K.Rutledge, *Low earth orbital atomic oxygen simulation for materials durability evaluation.* Proceedings of the Fourth European Symposium on Spacecraft Materials in the Space Environment,, 1988: p. 371–392.
5. Ferguson D. C. *The energy dependence and surface morphology of Kapton degradation under atomic oxygen bombardment*. in *Proc. 13th Space Simulation Conf.: The Payload-Testing for Success*. 1984. Orlando, FL.
6. Bruce A. Banks, Kim K. de Groh, and Sharon K. Miller, *MISSE Scattered Atomic Oxygen Characterization Experiment*, in *MISSE Post-Retreival Conference*. 2006: Orlando, Florida.
7. de Rooij, A., *The Oxidation of Silver by Atomic Oxygen.* ESA Journal, 1989. **13**.
8. A. R. Chambers, I. L. Harris, and G. T. Roberts, *Reactions of spacecraft materials with fast atomic oxygen.* Materials Letters, 1996. **26**: p. 121-131.
9. Sharon K.R. Miller, Bruce A. Banks, and Deborah L. Waters. *INVESTIGATION INTO THE DIFFERENCES IN ATOMIC OXYGEN*

EROSION YIELDS OF MATERIALS IN GROUND BASED FACILITIES COMPARED TO THOSE IN LEO. in *Proc. of the 10th ISMSE & the 8th ICPMSE*. 2006. Collioure, France.
10. J. B. Cross, et al., *Atomic oxygen-MoS2 chemical interactions*. Surf. Coat. Technol. 42, 1990.
11. B. Banks, T. Stueber, and M. Norris, *Monte Carlo Computational Modeling of the Energy Dependence of Atomic Oxygen Undercutting of Protected Polymers*, in *Fourth International Space Conference, ICPMSE-4*. 1998: Toronto, Canada.
12. Bruce A. Banks, et al. *Comparison of Atomic Oxygen Erosion Yields of Materials at Various Energies and Impact Angles*. in *Proc. of the 10th ISMSE & the 8th ICPMSE*. 2006. Collioure, France.
13. Leger, L.J., *Oxygen Atom Reaction with Shuttle Materials at Orbital Altitudes.* NASA TM 58246, 1982.
14. Peterson, P.N., R.C. Linton, and E.R. Miller, *Results of Apparent Atomic Oxygen Reactions on Ag, C, and Os Exposed During the Shuttle STS-4 Orbits.* Geophysical Research Letters, 1983. **10**: p. 569-571.
15. de Rooij, A. *THE DEGRADATION OF METAL SURFACES BY ATOMIC OXYGEN*. in *Proceedings of the Third European Symposium on Spacecraft Materials in Space Environment*. 1985. Noordwijk, The Netherlands,.
16. J. Kleiman, et al. *CO2-LASER ASSISTED ATOMIC OXYGEN BEAM SOURCES: RESEARCH, DEVELOPMENT AND OPTIMIZATION OF OPERATIONAL PARAMETERS*. in *Proc. of the 10th ISMSE & the 8th ICPMSE*. 2006. Collioure, France.

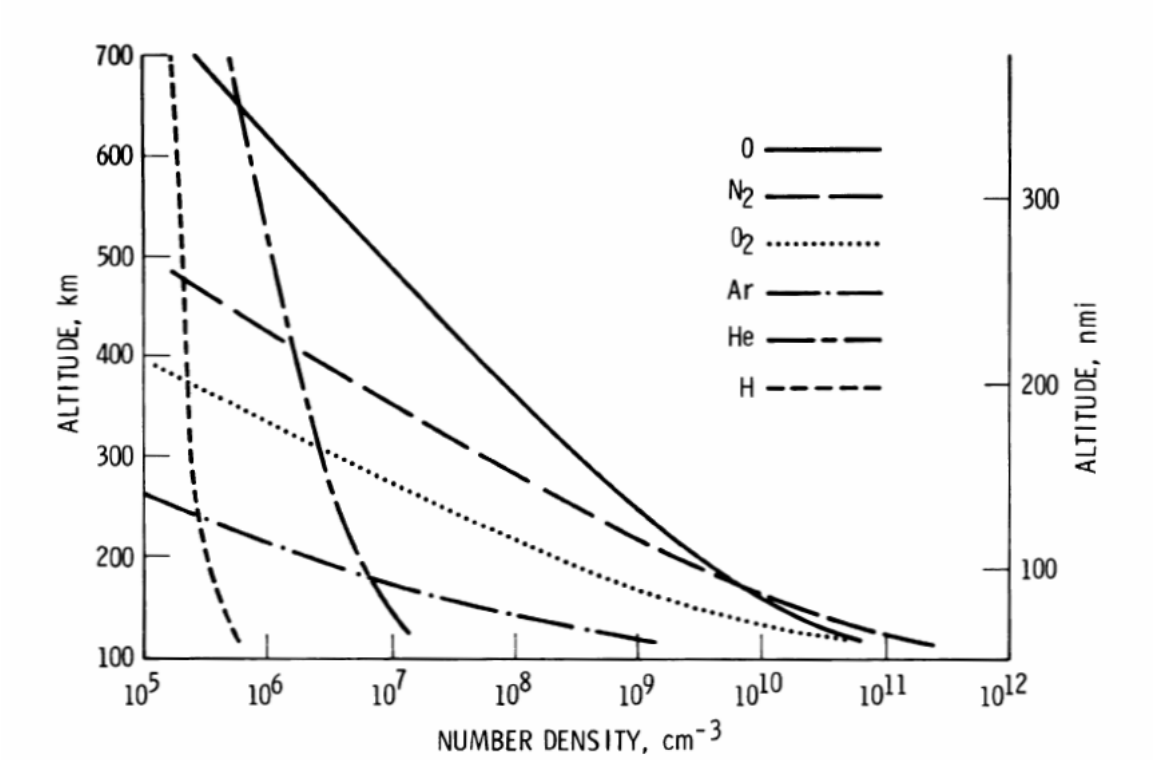

Figure 1: Atmospheric composition in Low Earth Orbit

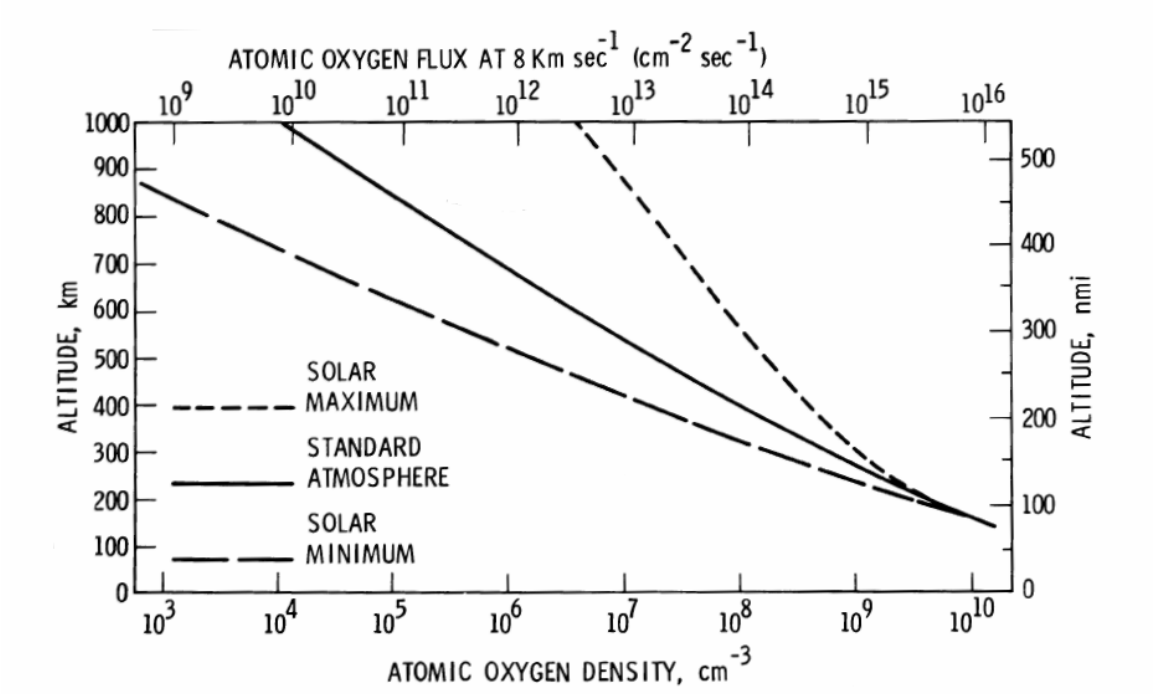

Figure 2: Atmospheric Atomic Oxygen density in Low Earth Orbit

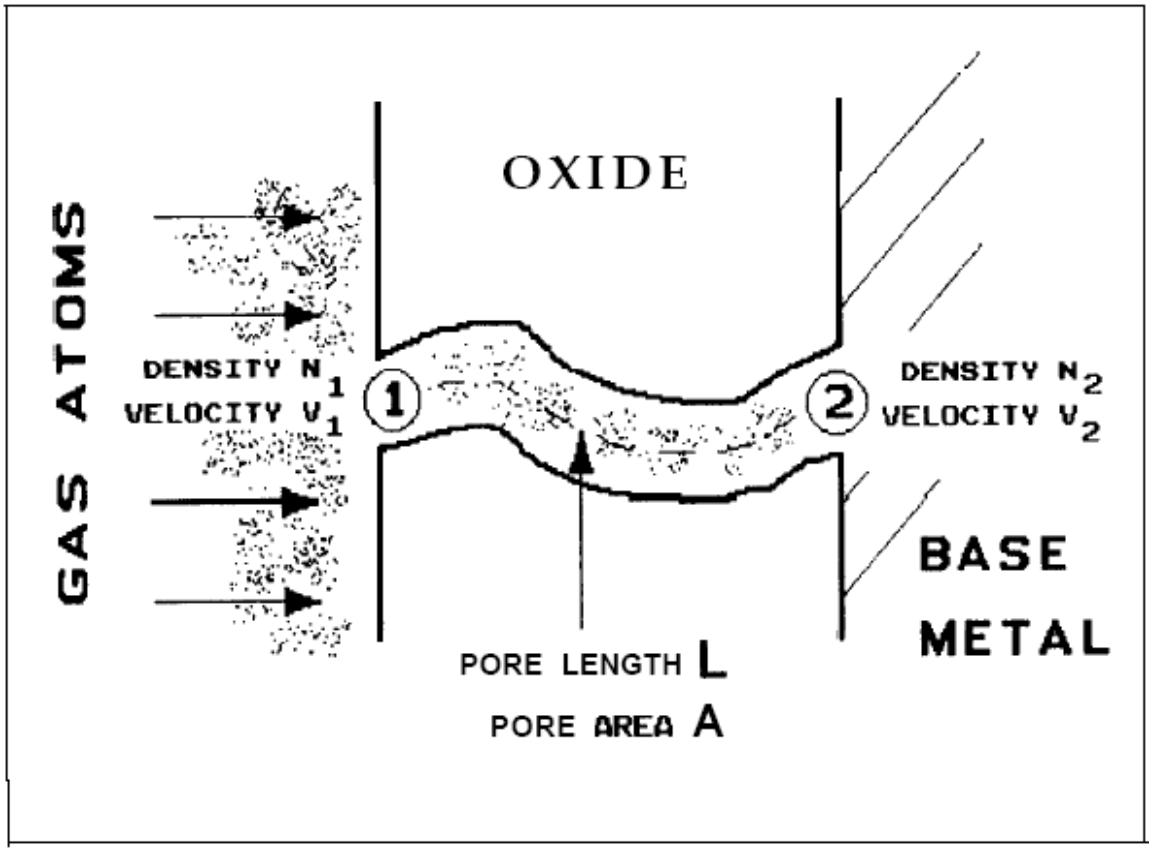

Figure 3: Model of oxide layer with pore

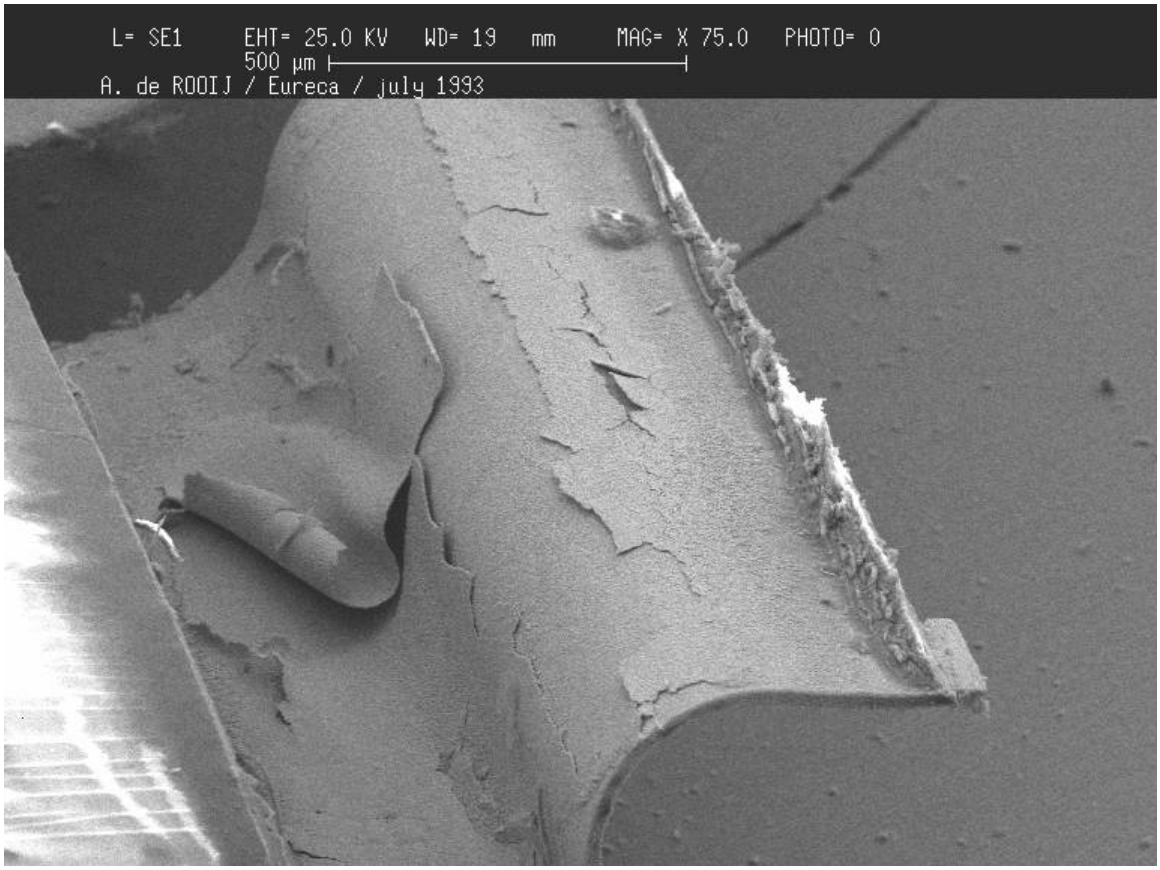

Figure 4: Silver interconnector (25 µm) retrieved from Eureca. It shows oxidised silver which is flaked off and exposing the underlying fresh material which is oxidised again.

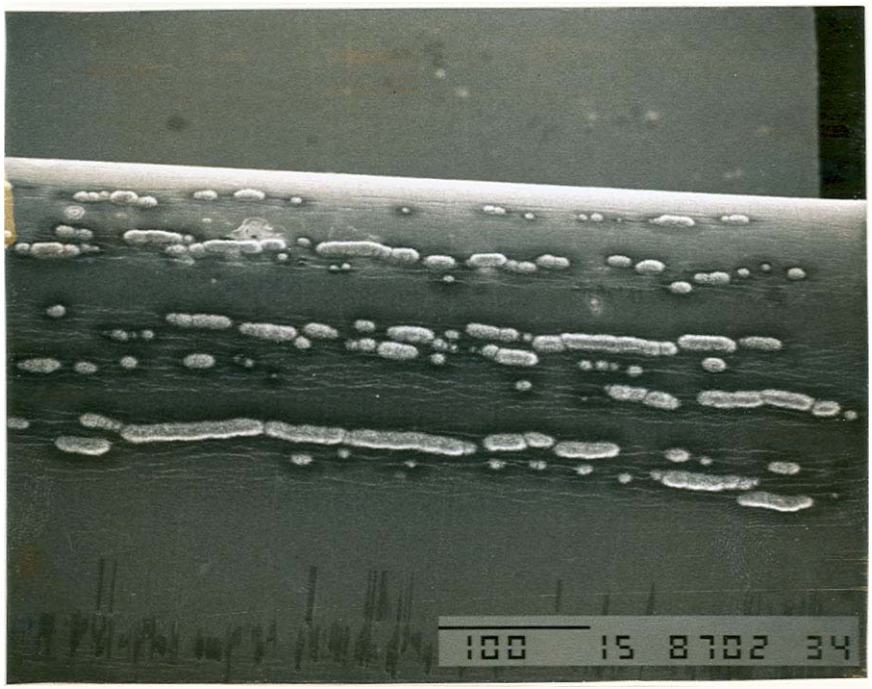

Figure 5: Gold coated silver is subjected to bending where after it is exposed to atomic oxygen. The horizontal artefacts are oxidised silver through defects in the gold plating.

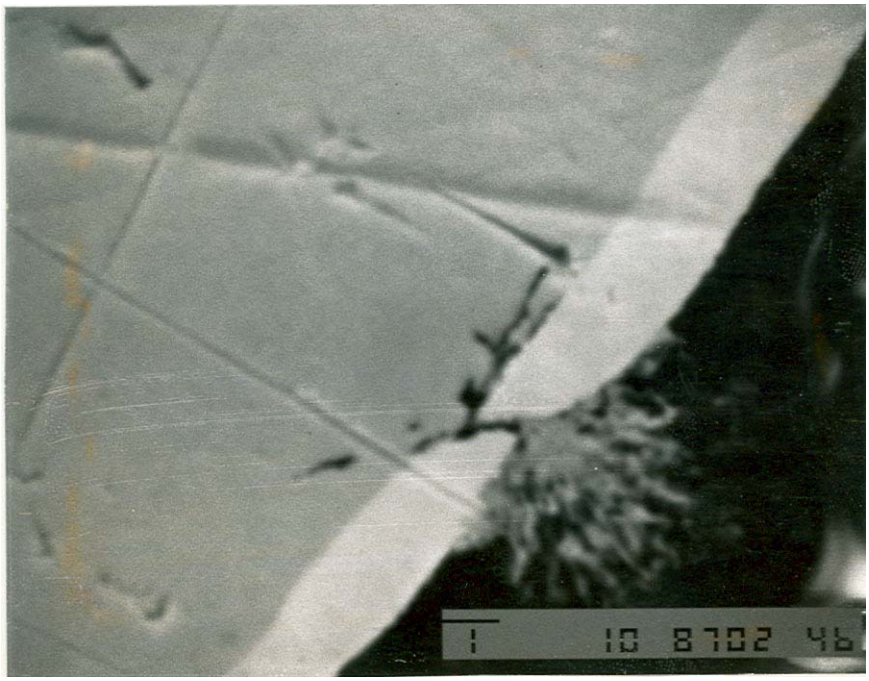

Figure 6: A microsection through a defect in the gold plating. It shows that silver is also attacked under the gold plating.